costimulates primary allogeneic proliferative responses and cytotoxicity mediated by small, resting T lymphocytes. *J. Exp. Med.* **175,** 353–360 (1992).
22. Kagi, D. *et al.* Fas and perforin pathways as major mechanisms of T cell-mediated cytotoxicity. *Science* **265,** 528–530 (1994).
23. Brunner, T. *et al.* Cell-autonomous Fas (CD95)/Fas-ligand interaction mediates activation-induced apoptosis in T-cell hybridomas. *Nature* **373,** 441–444 (1995).
24. Dhein, J., Walczak, H., Baumler, C., Debatin, K.-M. & Krammer, P. H. Autocrine T-cell suicide mediated by APO-1/(Fas/CD95). *Nature* **373,** 438–441 (1995).
25. Ju, S.-T. *et al.* Fas(CD95)/FasL interactions required for programmed cell death after T-cell activation. *Nature* **373,** 444-448 (1995).
26. Jäättela, M., Benedict, M., Tewari, M., Shayman, J. A. & Dixit, V. M. Bcl-x and Bcl-2 inhibit TNF and Fas-induced apoptosis and activation of phospholipase A_2 in breast carcinoma cells. *Oncogene* **10,** 2297–2305 (1995).
27. Subramanian, T., Kuppuswamy, M., Mak, S. & Chinnadurai, G. Adenovirus *cyt*$^+$ locus, which controls cell transformation and tumorigenicity, is an allele of *lp*$^+$ locus, which codes for a 19-kilodalton tumor antigen. *J. Virol.* **52,** 336–343 (1984).
28. Babiss, L. E., Fisher, P. B. & Ginsberg, H. S. Effect on transformation of mutations in the early region 1b-encoded 21- and 55-kilodalton proteins of adenovirus 5. *J. Virol.* **52,** 389–395 (1984).
29. Ranheim, T. S. *et al.* Characterization of mutants within the gene for the adenovirus E3 14.7-kilodalton protein which prevents cytolysis by tumor necrosis factor. *J. Virol.* **67,** 2159–2167 (1993).
30. Tripp, R. A., Hou, S., McMickle, A., Houston, J. & Doherty, P. C. Recruitment and proliferation of CD^{8+} T cells in respiratory virus infections. *J. Immunol.* **154,** 6013–6021 (1995).

Acknowledgements. We thank J. Freeman for help with the confocal microscopy, V. Dixit for the MCF7 and MCF7-Fas cell lines and for pcDNA-3-Fas, M. Green for the pMT2 vector, the ERp72 antiserum, and COS7 cells, M. Green for the DBP antiserum, M. Fukuda for LAMP1 antiserum, E. Harlow for the M73 mAb, C. Gugliemo for technical assistance, J. Mikes for preparation of the manuscript and figures, and C. Pollack for photography.

Correspondence and requests for materials should be addressed to W.S.M.W. (e-mail: woldws@slu.edu).

Integrin binding and mechanical tension induce movement of mRNA and ribosomes to focal adhesions

Marina E. Chicurel*†, Robert H. Singer†, Christian J. Meyer* & Donald E. Ingber*

* *Departments of Surgery and Pathology, Children's Hospital and Harvard Medical School, 300 Longwood Avenue, Boston, Massachusetts 02115, USA*
† *Department of Anatomy and Structural Biology, Albert Einstein College of Medicine of Yeshiva University, Bronx, New York 10461, USA*

The extracellular matrix (ECM) activates signalling pathways that control cell behaviour by binding to cell-surface integrin receptors and inducing the formation of focal adhesion complexes (FACs)[1,2]. In addition to clustered integrins, FACs contain proteins that mechanically couple the integrins to the cytoskeleton[3] and to immobilized signal-transducing molecules[1,2]. Cell adhesion to the ECM also induces a rapid increase in the translation of pre-existing messenger RNAs[4,5]. Gene expression can be controlled locally by targeting mRNAs to specialized cytoskeletal domains[6]. Here we investigate whether cell binding to the ECM promotes formation of a cytoskeletal microcompartment specialized for translational control at the site of integrin binding. High-resolution *in situ* hybridization revealed that mRNA and ribosomes rapidly and specifically localized to FACs that form when cells bind to ECM-coated microbeads. Relocation of these protein synthesis components to the FAC depended on the ability of integrins to mechanically couple the ECM to the contractile cytoskeleton and on associated tension-moulding of the actin lattice. Our results suggest a new type of gene regulation by integrins and by mechanical stress which may involve translation of mRNAs into proteins near the sites of signal reception.

FACs containing β1 integrin, talin, actin and vinculin could be visualized along the bead–membrane interface 20 min after human umbilical vein endothelial cells had bound to microbeads (4.5 μm) coated with fibronectin (FN) (Fig. 1a–f)[2,7]. High-resolution *in situ* hybridization using oligonucleotide probes for poly(A)$^+$ and ribosomal RNAs revealed that both mRNA and ribosomes were simultaneously recruited to the region surrounding the FAC (Fig. 1g–j). Whereas most FAC-associated cytoskeleton (CSK) proteins were

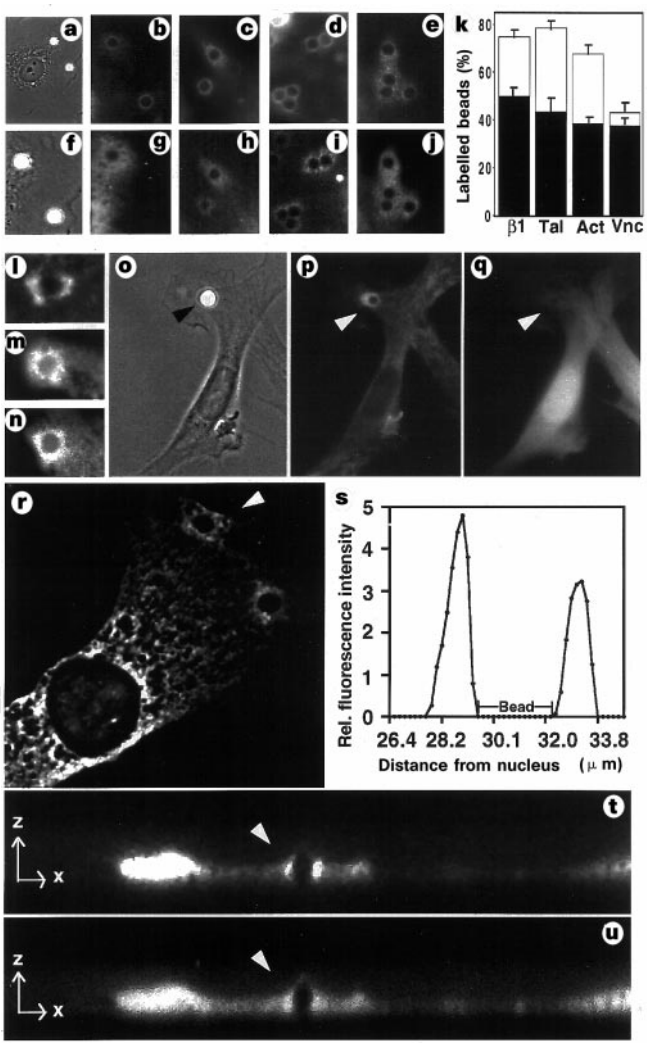

Figure 1 Recruitment of mRNA and ribosomes to FACs 20 min after cell binding to ECM-coated microbeads. Low- (**a**) and high- (**f**) magnification phase-contrast micrographs of a cell 20 min after binding to FN-coated beads. Fluorescence views showing immunostaining for β1 integrin (**b**) and *in situ* hybridization for ribosomal RNA (**g**) in the same cell as shown in **f**; bead diameter, 4.5 μm. Immunofluorescence staining for other FAC proteins, including talin (**c**), actin (**d**), and vinculin (**e**), in similarly treated cells. Corresponding *in situ* hybridization results obtained in the same cells using probes for poly(A)$^+$ (**h**, **i**) or ribosomal RNA (**j**) are shown below. **k**, Graph showing the percentage of beads that exhibited positive staining for each of the FAC proteins (white bars) and the subset of these beads that also stained positive for either poly(A)$^+$ RNA or ribosomes (black bars). β1, β1 integrin; Tal, talin; Act, actin; Vnc, vinculin. Error bars indicate s.e.m. Similar recruitment of mRNA was observed in human microvascular lung endothelial cells (**l**), bovine capillary endothelial cells (**m**), and NIH3T3 fibroblasts (**n**) bound to RGD-beads, as detected using an FITC-labelled oligo(dT) probe. Phase contrast (**o**) and corresponding fluorescence (**p**, **q**) views of a 3T3 fibroblast expressing high levels of soluble cytoplasmic enhanced green fluorescent protein through transfection. Binding to an RGD-coated bead (arrowheads) specifically induced recruitment of ribosomes (**p**) but not the green fluorescent protein (**q**). **r**, Digital imaging optical section in the *x*, *y* (horizontal) plane showing fluorescence staining for ribosomes in an endothelial cell bound to two FN-coated microbeads. **s**, Graph showing the relative fluorescence intensity in a single optical section due to ribosomal staining in the region of the cytoplasm surrounding one of the FN-coated beads shown in **r** (arrowhead). The average relative fluorescence intensity in a nearby cytoplasmic region at an equal distance from the nucleus in the same cell, but without an attached bead, was ~0.57 ± 0.67 in this study. Confocal micrographs in the *x*, *z* (vertical) plane showing fluorescence staining for poly(A)$^+$ RNA (**t**) and ribosomes (**u**) in a spread endothelial cell bound to a FN-coated microbead. Arrowheads indicate increased densities of poly(A)$^+$ RNA and ribosomes at the site of bead binding.

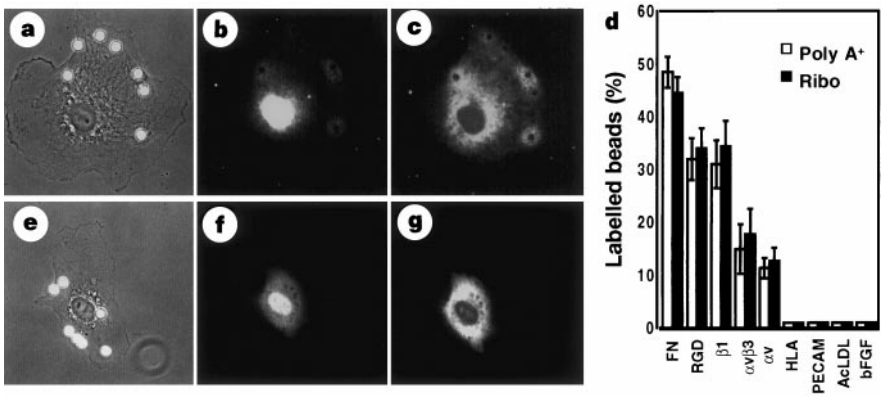

Figure 2 Integrin-dependent relocalization of poly(A)$^+$ RNA and ribosomes to the FAC at 20 min after bead binding. Phase contrast (**a**, **e**) and corresponding fluorescence (**b**, **c**, **f**, **g**) images of cells bound to beads coated with antibodies against integrin β1 (**a–c**) or FGF protein (**e–g**) and stained with an FITC-labelled oligo(dT) probe (**b**, **f**) or a Cy3-labelled ribosomal probe (**c**, **g**). Note that the FGF-coated beads that are incapable of inducing FAC formation show no bead-associated staining. **d**, Quantification of the percentage of beads that stained positively for poly(A)$^+$ RNA and ribosomes within cells bound to beads coated with FN (FN); RGD peptide (RGD); antibodies against β1 integrin (β1), αvβ3 integrin (αvβ3), αv integrin (αv), HLA histocompatibility antigen (HLA), or PECAM; or with the metabolic receptor ligands, acetylated low-density lipoprotein (AcLDL) or FGF.

restricted to the bead–membrane interface, mRNA and ribosomes appeared to form larger amorphous haloes that encompassed the FAC and extended farther into the cytoplasm (~2.5 μm) at this time. Vinculin gave a similar diffuse staining pattern (Fig. 1e, j). Quantification of staining at this time (20 min after bead binding) revealed that only a subset of beads recruited FAC proteins[2,7] and that only a subset of these FACs stained positively for mRNA or ribosomes (Fig. 1k). However, beads labelled for mRNA almost invariably contained FAC proteins. Similar results were obtained using beads coated with RGD peptide and with other cell types (Fig. 1l–n). In contrast, specific staining was not observed when fixed cells were pretreated with RNAse before hybridization or when a 'sense' oligo(dA) probe was used instead of oligo(dT). Furthermore, soluble cytoplasmic components, such as transfected green fluorescent protein (GFP), did not appear to accumulate around bead-induced FACs (Fig. 1o–q). Digital imaging microscopy in the *x*, *y* plane (Fig. 1r, s) and confocal microscopy in the *x*, *z* plane (Fig. 1t, u) confirmed that the local densities of ribosomes and poly(A)$^+$ RNA were indeed specifically increased in the region of the bead-associated FAC.

Different integrin subtypes differed in their ability to promote poly(A)$^+$ RNA and ribosome redistribution. Beads coated with anti-integrin β1 antibodies (Fig. 2a–c) induced more mRNA and ribosome relocation than did beads coated with either anti-αvβ3 or anti-α*v* antibodies (Fig. 2d). In contrast, beads coated with ligands for other (non-integrin) transmembrane receptors, including specific antibodies (against HLA antigen, or PECAM) or metabolic receptor ligands, such as basic fibroblast growth factor (FGF) or acetylated low-density lipoprotein, failed to induce any visible recruitment (Fig. 2d–g). Thus, the observed relocation of mRNA and ribosomes in response to ECM binding appeared to be specifically mediated by integrin binding and associated FAC formation.

In migrating fibroblasts, β-actin mRNA localizes to the CSK at the leading edge within a few minutes of growth factor stimulation[8]. Similarly, staining for poly(A)$^+$ RNA and ribosomes could be detected delineating the bead–membrane interface within the FAC 5 min after bead binding; the staining pattern only later became more diffuse and extended into the surrounding cytoplasm (Fig. 3a). The percentage of positively stained beads also progressively increased over time, saturating at ~20 min after bead binding (Fig. 3a). These rapid kinetics suggested that transcription and nuclear transport might not be required for RNA localization to FACs. To test this, we enucleated cells to produce cytoplasts and then allowed them to bind to FN-coated beads (Fig. 3b–d). The percentage of beads that exhibited recruitment of poly(A)$^+$ RNA and ribosomes was nearly identical in nucleated cytoplasts and

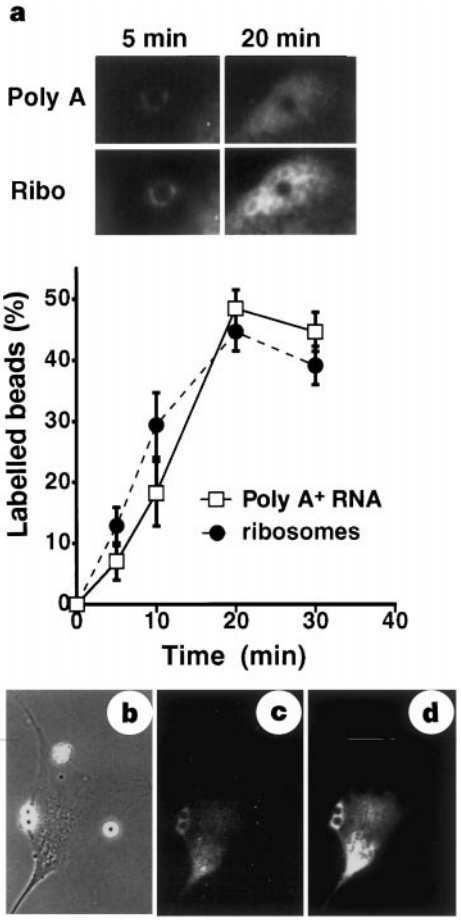

Figure 3 Kinetics of mRNA and ribosome recruitment to the FAC. **a**, Top, fluorescence staining for poly(A)$^+$ RNA (Poly A) and ribosomes (Ribo) around a cell-surface-bound FN-coated bead at 5 and 20 min after binding. Graph shows time course of recruitment of poly(A)$^+$ RNA and ribosomes to the FAC. Phase-contrast (**b**) and corresponding fluorescence views (**c**, **d**) of an enucleated cytoplast bound to FN-coated beads that stained positively for poly(A)$^+$ RNA (**c**) and ribosomes (**d**).

control cells (34.25 ± 4.97 compared with 36.63 ± 1.92, respectively). Thus, neither *de novo* synthesis of RNA nor vectorial transport of RNA from the nucleus to the cytoplasm was required for the repositioning of poly(A)$^+$ RNA and ribosomes to the FAC.

Compartmentalization of specific mRNAs observed in many cell types, including oocytes, neurons, muscle cells and fibroblasts, appears to be mediated by the targeting of existing cytoplasmic mRNAs to specific microdomains of the insoluble CSK[6]. In fact, disruption of the actin lattice using cytochalasin D blocked recruitment of poly(A)$^+$ RNA and ribosomes to the FAC in our cells (Fig. 4a). In contrast, treatment of cells with microtubule-modifying drugs, such as nocodazole and taxol, had only minimal effects. Poly(A)$^+$ RNA could therefore be passively recruited to the FAC owing to its association with actin filaments[9], which accumulate at the bead surface as the cell extends ruffles around the bead in response to integrin binding (Fig. 4b, c). We consider this unlikely, however, because beads that stained positively for actin were negative or very dimly stained for poly(A)$^+$ RNA and ribosomes and vice versa (Fig. 4b–d).

Another possibility is that this microcompartmentalization is controlled mechanically through tension-dependent restructuring of the CSK. For example, certain mRNAs preferentially associate with vertices in the actin lattice and not with the intervening struts[10]. These fine microarchitectural features can be generated through changes in isometric tension resulting from cell binding to an ECM substrate that can resist cell-tractional forces[11]. If tension-moulding of the CSK is required for the observed redistribution of the protein synthesis machinery, then changing the balance of forces transmitted across the cell surface, for example by altering mechanical coupling between integrins and the CSK, should modify this recruitment response. We found that there was a direct correlation between the ability of transmembrane receptors to cause mRNA and ribosomes to relocalize to the FAC and their ability to resist mechanical distortion, as previously demonstrated using magnetic twisting cytometry[12]. Beads that formed the strongest CSK attachments (coated with RGD peptide or anti-β1 integrin antibodies) were consistently more effective at inducing recruitment than beads coated with receptor ligands which gave intermediate (anti-αvβ3 and anti-αv antibodies) or low (AcLDL, anti-HLA) levels of mechanical coupling to the CSK (Fig. 2). Furthermore, treatment of cells with drugs such as KT5926 and butanedione-2-monoxime (BDM) that inhibit actomyosin-based tension generation without disrupting CSK filaments[13,14] also decreased recruitment of poly(A)$^+$ RNA and ribosomes to the FAC (Fig. 4a). Finally, we could directly demonstrate that tension *per se* is a trigger for these repositioning events by applying mechanical stresses to cell surface integrin receptors using controlled magnetic twisting forces and cell magnetometry[3]. Application of mechanical stresses ranging from 0 to 15 dynes cm^{-2} to cell-surface-bound magnetic beads coated with RGD peptide resulted in a stress-dependent increase in the percentage of beads that stained for ribosomes after 5 min stress application (Fig. 4e). Myosin V is required for the transport of *ASH1* mRNA in budding yeast[15] and localization of β-actin mRNA to the leading edge appears to involve the small GTP-binding protein Rho (V. Latham and R.H.S., unpublished results), which promotes FAC formation by increasing myosin light-chain phosphorylation and increasing CSK tension[16]. These results indicate that cell adhesion to the ECM and integrin binding may create a specialized microcompartment containing mRNA and ribosomes near the FAC through mechanical restructuring of the surrounding actin lattice and the corresponding formation of geometries that promote mRNA and ribosome binding (Fig. 4f).

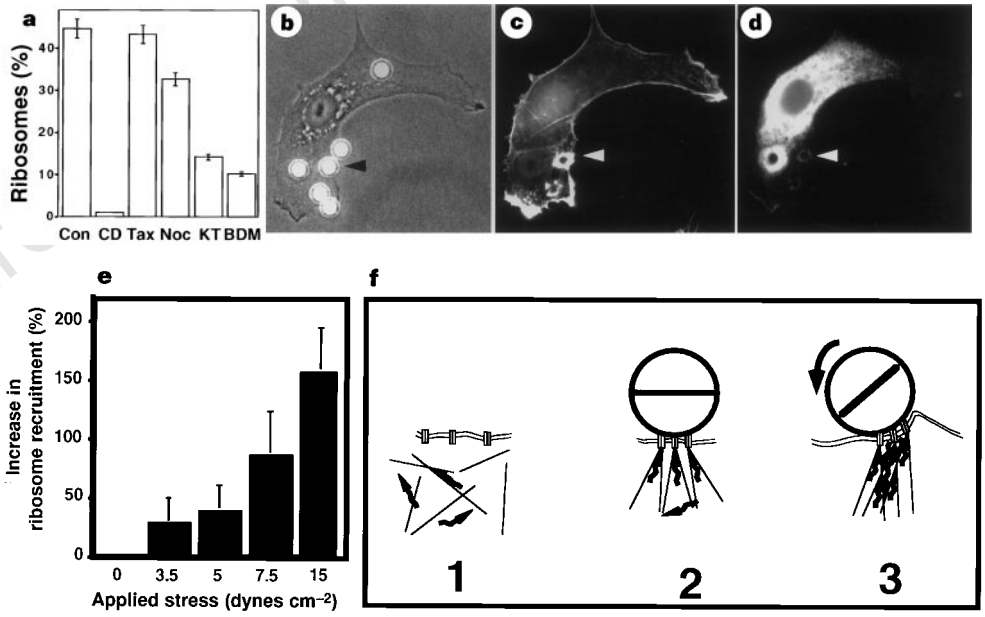

Figure 4 The role of the CSK and mechanical tension in the recruitment process. **a**, Percentage of beads that recruited ribosomes in control untreated cells (Con) or in cells treated for 30 min with 1 μg ml^{-1} cytochalasin D (CD), 1 μM Taxol (Tax), or 10 μg ml^{-1} nocodazole (Noc) or for 1 h with 15 μM KT5926 (KT) or 20 mM BDM. Phase contrast (**b**) and corresponding fluorescence views (**c**, **d**) of the same cell bound to FN-coated beads stained for F-actin using FITC-phalloidin (**c**) or ribosomes (**d**). Arrowhead indicates a bead that is brightly stained for F-actin but only dimly stained for ribosomes, whereas the adjacent bead to the left is only weakly stained with phalloidin but brightly stained for ribosomes. **e**, Mechanical-stress-dependent recruitment of ribosomes to the FAC. Rotational shear stresses ranging from 0 to 15 dynes cm^{-2} were applied to cell-surface-bound magnetic beads coated with RGD peptide using controlled magnetic twisting forces[3]. Error bars indicate s.e.m. **f**, Model of tension-dependent recruitment of mRNA and ribosomes to the FAC. Integrin receptors (rectangles) on the cell membrane (1) are induced to cluster and form a FAC linked to the actin CSK (black lines) in response to binding to a FN-coated bead (large circle) (2). The ability of the bound bead to resist CSK tension results in a low level of CSK reorganization that exposes sites that promote binding of ribosomes and mRNA (arrows) previously present within the cytoplasm (2). Increasing the level of mechanical distortion within the actin lattice by magnetically twisting the bound beads results in progressive tension-moulding of the lattice, creation of additional binding sites, and thus enhanced recruitment of mRNA and ribosomes to the site of integrin binding (3). This restructuring and microcompartmentalization starts at the bead–membrane interface and then progressively extends outwards into the cytoplasm, as in Fig. 3.

Our results suggest that rapid post-transcriptional changes in gene expression may be mediated by repositioning of translational components to sites of signal reception and that mechanical tension may guide these movements. FACs contain several signal-transducing molecules, including proteins that can regulate translation (the Na^+/H^+ antiporter[1,17,18], protein kinase C[19–21], PI-3 kinase[1,2,22] and the FGF receptor[1,23], for example). Thus, redistribution of mRNA and ribosomes to the FAC may explain the rapid increase in protein synthesis that is observed well before changes in transcription are detectable in response to substrate adhesion[4]. Other FAC components, such as calreticulin[24] and proteins containing LIM domains (such as zyxin, cysteine-rich protein-1 and paxillin)[25], can potentially bind nucleic acids and may thus also play a role in the observed response to stress and integrin binding. Formation of this localized complex could also mediate the post-transcriptional effects of mechanical stresses on gene expression. For example, in cardiocytes, an acute rise in ventricular wall stress results in a rapid increase in protein synthesis and phosphorylation of the translation initiation factor eIF-4E, effects that can be prevented by treatment with BDM[26]. These observations suggest that translation of gene products at the site of ECM signal reception may constitute a novel aspect of integrin signalling and serve an intermediate role between rapid local post-translational changes (such as tyrosine phosphorylation, local CSK rearrangements) and slower transcriptional alterations in the nucleus. Formation of this microcompartment for post-transcriptional control of gene expression also may serve to integrate signals that regulate cellular protein synthesis with those that are elicited by integrins, growth-factor receptors and mechanical stresses within the same FAC[1–3]. □

Methods

Cell culture. Endothelial cells from human umbilical vein[27], bovine adrenal cortex[17], or human lung microvasculature (Clonetics) and NIH3T3 cells were cultured on FN-coated glass coverslips in serum-containing medium for 14–16 h before bead addition. NIH3T3 cells were transfected with a plasmid encoding an enhanced green fluorescent protein (Clontech) using lipofectamine (GIBCO-BRL). Cytoplasts were generated[28] and incubated with beads 3 h after cytochalasin B washout. Polystyrene beads (4.5 μm; Polysciences) were coated with FN (Cappel), AcLDL (Biomedical Technologies), FGF (Takeda Chemical), RGD-containing peptide (Peptide 2000; Telios) or rabbit anti-mouse IgG (Cappel) as described[29]. Beads coated with anti-IgG were incubated with purified antibodies (25 μg ml^{-1}) to HLA (clone W 6-32, ATCC), PECAM (clone P2B1, Chemicon), or integrin types β1 (clone B-D15, Biosource), αvβ3 (clone LM609, Chemicon), or αv (clone P3G8, Chemicon). Beads were added to cells (30 beads per cell) in serum-free medium with 1% BSA, washed free of unattached beads, and fixed in paraformaldehyde. Uncoated beads, beads coated only with anti-mouse IgG antibodies, or beads coated with antibodies directed against intracellular proteins did not bind to cell surfaces.

***In situ* hybridization.** *In situ* hybridization was performed using probes directly labelled with either FITC or Cy3 fluorochromes as described[30]. An oligo(dT) 43-mer was used to assess poly(A)$^+$ RNA distribution; an oligo(dA) 43-mer was used as a negative control. Ribosomes were detected using a mixture of 4 oligonucleotide probes complementary to the human 18S ribosomal RNA (all 5′ to 3′: ACGGTATCTGATCGTCTTCGAACCTCCGACT; ACCCGCACTTACTGGGAATTCCTCGTTCAT; TTATTCGTCAATCTCGGGTGGCTGAACGCCACTT; GCCTCACTAAACCATCCAATCGGTAGTAGC). An anti-ribosomal antibody produced similar results. Hybridizations were carried out at 37 °C for 2 h in 10% (oligo(dT) probes) or 30% formamide (ribosomal probes). The highest stringency washes were performed at 37 °C in 1× SSC, 10% formamide (for oligo(dT) probes) or 30% formamide (for ribosomal probes). Quantitative data are expressed as the pooled average of more than 230 beads obtained from at least two independent experiments.

Immunofluorescence. Immunofluorescence microscopy was performed as described[7] using antibodies at the following dilutions: anti-β1 integrin (clone B-D15, Biosource) 1:40, anti-talin (Chemicon) 1:25, anti-vinculin (clone hVIN-1, Sigma) 1:400, and anti-ribosomal P antigen (Immunovision) 1:50, FITC-labelled sheep anti-mouse IgG (Amersham) 1:50, Cy3-labelled goat anti-mouse IgG (Amersham) 1:1,000, and biotin-labelled goat anti-human IgG (Vector) 1:200. FITC- or Texas red-labelled avidin D (Vector) was used at a dilution of 1:250 and FITC-labelled phalloidin (Sigma) at 1:100. A Leica TCS4D confocal microscope was used to obtain optical sections in the vertical (x, z) plane. Digital (deconvolution) imaging microscopy was used to obtain horizontal (x, y) optical sections and to quantify relative fluorescence intensities[9].

Magnetic twisting cytometry. Mechanical stresses were applied directly to cell-surface integrin receptors by magnetically twisting surface-bound ferromagnetic beads (4.5 μm; Spherotech) that were coated with RGD peptide[3]. A 1,000 gauss magnetic field was first applied for 10 μs to align the moments of the beads 5 min after binding to the cell surface and then 0–30 gauss magnetic fields were applied in an orthogonal direction for 5 more minutes to exert a controlled shear stress (torque) to the beads bound to cell-surface receptors.

Received 24 September 1997; accepted 3 February 1998.

1. Plopper, G., McNamee, H. P., Dike, L. E., Bojanowski, K. & Ingber, D. Convergence of integrin and growth factor receptor signaling pathways within the focal adhesion complex. *Mol. Biol. Cell.* **6,** 1349–1365 (1995).
2. Miyamoto, S. *et al.* Integrin function: molecular hierarchies of CSK and signaling molecules. *J. Cell Biol.* **131,** 791–805 (1995).
3. Wang, N. J., Butler, P. & Ingber, D. E. Mechanotransduction across the cell surface and through the CSK. *Science* **260,** 1124–1127 (1993).
4. Benecke, B.-J., Ben-Ze'ev, A., Benecke, B.-J. & Penman, S. The control of mRNA production, translation and turnover in suspended and reattached anchorage-dependent fibroblasts. *Cell* **14,** 931–939 (1978).
5. Farmer, S. R., Ben-Ze'ev, A. & Penman, S. Altered translatability of messenger RNA from suspended anchorage-dependent fibroblasts: reversal upon cell attachment to a surface. *Cell* **15,** 627–637 (1978).
6. Bassell, G. & Singer, R. H. mRNA and cytoskeletal filaments. *Curr. Opin. Cell Biol.* **9,** 109–115 (1997).
7. Plopper, G. & Ingber, D. E. Rapid induction and isolation of focal adhesion complexes. *Biochem. Biophys. Res. Commun.* **193,** 571–578 (1993).
8. Latham, V., Kislauskis, E., Singer, R. & Ross, A. β-Actin mRNA localization is regulated by signal transduction mechanisms. *J. Cell Biol.* **126,** 1211–1219 (1994).
9. Taneja, K. L., Lifshitz, L. M., Fay, F. S. & Singer, R. H. Poly(A) RNA codistribution with microfilaments: Evaluation by *in situ* hybridization and quantitative digital imaging microscopy. *J. Cell Biol.* **119,** 1245–1260 (1992).
10. Bassell, G. J., Powers, C. M., Taneja, K. L. & Singer, R. H. Single mRNAs visualized by ultrastructural in situ hybridization are principally localized at actin filament intersections in fibroblasts. *J. Cell Biol.* **126,** 863–876 (1994).
11. Ingber, D. E. Cellular tensegrity: defining new rules of biological design that govern the cytoskeleton. *J. Cell Sci.* **104,** 613–627 (1993).
12. Wang, N. & Ingber, D. E. Probing transmembrane mechanical coupling and cytomechanics using magnetic twisting cytometry. *Biochem. Cell Biol.* **73,** 327–335 (1995).
13. Cramer, L. P. & Mitchison, T. J. Myosin is involved in postmitotic cell spreading. *J. Cell Biol.* **131,** 179–189 (1995).
14. Nakanishi, S., Yamada, K., Iwahashi, K., Kuroda, K. & Kase, H. KT5926, a potent and selective inhibitor of myosin light chain kinase. *Mol. Pharmacol.* **37,** 482–488 (1990).
15. Long, R. M. *et al.* Mating type switching in yeast controlled by asymmetric localization of ASH1 mRNA. *Science* **277,** 383–387 (1997).
16. Chrzanowska-Wodnicka, M. & Burridge, K. Rho-stimulated contractility drives the formation of stress fibers and focal adhesions. *J. Cell Biol.* **133,** 1403–1415 (1996).
17. Ingber, D. E. *et al.* Control of intracellular pH and growth by fibronectin in capillary endothelial cells. *J. Cell Biol.* **110,** 1803–1811 (1990).
18. Edmonds, B. T., Murray, J. & Condeelis, J. pH regulation of the F-actin binding properties of *Dictyostelium* elongation factor 1a. *J. Biol. Chem.* **270,** 15222–15230 (1995).
19. Vuori, K. & Ruoslahti, E. Activation of protein kinase C precedes α5β1 integrin-mediated cell spreading on FN. *J. Biol. Chem.* **268,** 21459–21462 (1993).
20. Morley, S. J. Signal transduction mechanisms in the regulation of protein synthesis. *Mol. Biol. Rep.* **19,** 221–231 (1994).
21. Whalen, S. G. *et al.* Phosphorylation of eIF-4E on serine 209 by protein kinase C is inhibited by the translational repressors, 4E-binding proteins. *J. Biol. Chem.* **271,** 11831–11837 (1996).
22. Von Manteuffel, S., Gingras, A. C., Ming, X. F., Sonenberg, N. & Thomas, G. 4E-BP1 phosphorylation is mediated by the FRAP-p70s6k pathway and is independent of mitogen-activated protein kinase. *Proc. Natl Acad. Sci. USA* **93,** 4076–4080 (1996).
23. Sonenberg, N. Regulation of translation and cell growth by eIF-4E. *Biochimie* **76,** 839–846 (1994).
24. Singh, N. K., Attreya, C. D. & Nakhasi, H. L. Identification of calreticulin as a rubella virus RNA binding protein. *Proc. Natl Acad. Sci. USA* **91,** 12770–12774 (1994).
25. Schmeichel, K. L. & Beckerle, M. C. Molecular dissection of a LIM domain. *Mol. Biol. Cell.* **8,** 219–230 (1997).
26. Wada, H., Ivester, C. T., Carabello, B. A., Cooper, G. & McDermott, P. J. Translational initiation factor eIF-4E. A link between cardiac load and protein synthesis. *J. Biol. Chem.* **271,** 8359–8364 (1996).
27. Kourembanas, S., Hannan, R. L. & Faller, D. V. Oxygen tension regulates the expression of the platelet-derived growth factor-B chain in human endothelial cells. *J. Clin. Invest.* **86,** 670–674 (1990).
28. Lucas, J. J., Szekely, E. & Kates, J. R. The regeneration and division of mouse L-cell karyoplasts. *Cell* **7,** 115–122 (1976).
29. Schwartz, M. A., Lechene, C. & Ingber, D. E. Insoluble FN activates the Na+/H+ antiporter by clustering and immobilizing integrin alpha 5 beta 1, independent of cell shape. *Proc. Natl Acad. Sci. USA* **88,** 7849–7853 (1991).
30. Zhang, G., Taneja, K. L., Singer, R. H. & Green, M. R. Localization of pre-mRNA splicing in mammalian nuclei. *Nature* **372,** 809–812 (1994).

Acknowledgements. We thank K. Taneja, S. Shenoy, N. Wang, J. Fredberg, S. Kourembanas, G. Lee, G. Whitesides and the Biomedical Imaging Facility at the University of Massachusetts in Worcester for key reagents, equipment and technical expertise, and B. Peters and C. Chen for discussion. This work was supported by grants from the NIH and NASA and an American Cancer Society postdoctoral fellowship.

Correspondence and requests for materials should be addressed to D.E.I. (e-mail: ingber@a1.tch.harvard.edu).